AGU PUBLICATIONS

Geophysical Research Letters

RESEARCH LETTER
10.1002/2016GL070346

Key Points:
- Lithological variations of mantle beneath southeastern China during Late Mesozoic are induced by the subduction of paleo-Pacific plate
- The subduction of paleo-Pacific plate can be responsible for the mantle-derived magmatism between approximately 150 Ma and 110 Ma in southeastern China
- The paleo-Pacific slab rollback with increased dip angle is a possible model to control the lithological variations of Late Mesozoic mantle

Supporting Information:
- Supporting Information S1

Correspondence to:
G. Zeng,
zgang@nju.edu.cn

Citation:
Zeng, G., Z.-Y. He, Z. Li, X.-S. Xu, and L.-H. Chen (2016), Geodynamics of paleo-Pacific plate subduction constrained by the source lithologies of Late Mesozoic basalts in southeastern China, *Geophys. Res. Lett.*, *43*, 10,189–10,197, doi:10.1002/2016GL070346.

Received 12 JUL 2016
Accepted 25 SEP 2016
Accepted article online 27 SEP 2016
Published online 11 OCT 2016

Geodynamics of paleo-Pacific plate subduction constrained by the source lithologies of Late Mesozoic basalts in southeastern China

Gang Zeng[1], Zhen-Yu He[2], Zhen Li[3], Xi-Sheng Xu[1], and Li-Hui Chen[1]

[1]State Key Laboratory for Mineral Deposits Research, School of Earth Sciences and Engineering, Nanjing University, Nanjing, China, [2]Institute of Geology, Chinese Academy of Geological Science, Beijing, China, [3]ARC Centre of Excellence for Core to Crust Fluid Systems (CCFS) and The Institute for Geoscience Research (TIGeR), Department of Applied Geology, Curtin University, Perth, Western Australia, Australia

Abstract Widespread Late Mesozoic volcanic magmatism in southeastern China is generally thought to represent products in response to the subduction of paleo-Pacific plate; however, it remains unclear when this process began to affect the mantle and the related magmatism. Here we present a systematic study on the source lithology of Late Mesozoic basalts in this area to highlight a link between lithological variations of mantle and subduction process of paleo-Pacific plate. Late Mesozoic basalts can be subdivided into four groups based on their erupted ages: 178~172 Ma, approximately 150 Ma, 137~123 Ma, and 109~64 Ma. The primary source lithology of these rocks is pyroxenite rather than peridotite, and this mafic lithology can be formed by either ancient or young recycled crustal components. Notably, the source lithology of the approximately 150 Ma and 137~123 Ma basalts is primarily SiO_2-rich pyroxenite, and the former is carbonated. The discovery of carbonated, SiO_2-rich pyroxenite reflects the influence of a recently recycling event in the mantle. The subduction of paleo-Pacific plate is the most appropriate candidate and can be responsible for the mantle-derived magmatism after approximately 150 Ma in southeastern China. Therefore, we suggest a paleo-Pacific slab rollback with increased dip angle as a possible model to control the lithological variations of Late Mesozoic mantle beneath southeastern China.

1. Introduction

Late Mesozoic volcanic magmatism is widespread in southeastern China and is generally attributed to the subduction of paleo-Pacific plate, although the petrogenesis and associated tectonic models remain controversial, including the normal subduction model [e.g., *Jahn et al*., 1990; *Klimetz*, 1983], the flat-slab subduction [e.g., *Li and Li*, 2007], and the subduction with variable angles [e.g., *Zhou and Li*, 2000; *Zhou et al*., 2006]. For the model of subduction with variable angles, approximately 110 Ma has been proposed to correspond to the transformation from low-angle forward to high-angle rollback subduction of the paleo-Pacific plate [*He and Xu*, 2012; *Meng et al*., 2012]. Up to now, we do not know when the subducted paleo-Pacific plate began to affect the mantle beneath southeastern China and the mantle-derived magmatism. Because the paleo-Pacific plate has subducted into the mantle, the studies on mantle-derived basaltic rocks can provide important information on potential interaction process between subducted plate and the mantle and therefore help us to understand the influence of paleo-Pacific subduction on the mantle.

Previous studies focus on the geochronology and geochemical compositions of Late Mesozoic basalts (especially the isotopic compositions) to document the potential genetic relationship between spatial and temporal distributions of basalts and the subduction of paleo-Pacific plate [e.g., *Chen et al*., 2008; *Meng et al*., 2012; *Wang et al*., 2008, 2003]. However, using isotopes to trace the magmatic process is sometimes difficult and might be ambiguous because different petrogenetic models can produce similar isotopic compositions of basalts. Recently, identification of source lithology provides us a new, efficient perspective to constrain the formation of basaltic magma and understand the characteristics of mantle and have been widely used in the studies of the oceanic basalts [e.g., *Dasgupta et al*., 2010; *Herzberg*, 2006, 2011; *Pilet et al*., 2008; *Sobolev et al*., 2007] and Cenozoic basalts from eastern China [e.g., *Wang et al*., 2011; *Xu et al*., 2012a, 2012b; *Zeng et al*., 2010, 2011]. Understanding the source lithology of mantle-derived rocks can also help us to constrain the crustal recycling (e.g., the subduction of oceanic slab) because this process would change the mantle

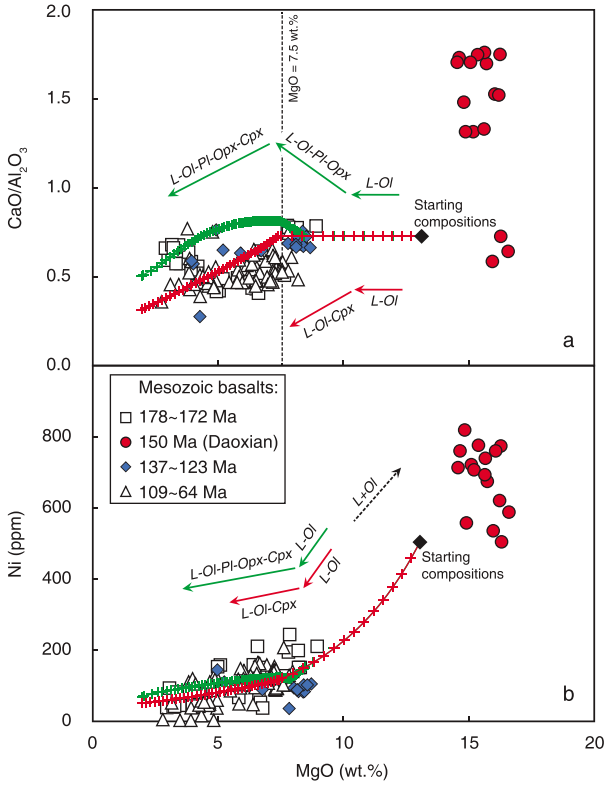

Figure 1. Variations in (a) CaO/Al_2O_3 and (b) Ni versus MgO for the Late Mesozoic basalts in southeastern China. Data for Late Mesozoic basalts in southeastern China are listed in Table S1 in the supporting information [*Chen et al.*, 2008; *Dai*, 2007; *Li et al.*, 2004; *Meng et al.*, 2012; *Wang et al.*, 2003; *Yang et al.*, 2015]. The green and red lines represent the fractionation of "ol + pl + opx + cpx" and "ol + cpx," respectively. The fractionation of different minerals are calculated by the software "Petrolog 3" [*Danyushevsky and Plechov*, 2011], using a calculated primary melt (07SC10-4) for Hengshan basalts, Rucheng Basin (Table S2), as the starting composition.

lithology. However, the source lithology for Late Mesozoic basalts in southeastern China is still poorly understood, and additional work is required before we can properly assess the genesis of these basalts. In this study, we show that the lithological variations of mantle source for Late Mesozoic basalts from southeastern China are related to the subduction of paleo-Pacific plate, which establishes a link between the evolution of the mantle source and the tectonic history of southeastern China during the Late Mesozoic.

2. Compositional Variations in Late Mesozoic Basalts

According to the nomenclature of *Le Bas et al.* [1986], Late Mesozoic mafic volcanic rocks from southeastern China are classified as basalts, trachybasalts, and basaltic andesites, with minor samples plotting in the area of basanites and basaltic trachyandesites (Figure S1 in the supporting information). Here we compiled geochemical data of these mafic rocks from southeastern China (Table S1 in the supporting information) and subdivided them into four groups based on their erupted ages: 178~172 Ma, approximately 150 Ma, 137~123 Ma, and 109~64 Ma (Figure S2). Most mafic rocks in southeastern China show continuous variations in major element compositions, except for the approximately 150 Ma Daoxian basalts. Daoxian basalts have obviously lower Al_2O_3, TiO_2, and Na_2O contents and higher MgO contents and higher CaO/Al_2O_3 ratios than other mafic rocks (Figure 1a; others not shown). Additionally, Daoxian basalts also show significantly higher Ni and Cr contents than other mafic rocks (Figure 1b; MgO versus Cr not shown). In a primitive-mantle-normalized incompatible element diagram (Figure S3), these Daoxian basalts are enriched in large-ion lithophile elements and light rare earth elements, with significantly positive Ba and negative Nb-Ta, Zr-Hf and Ti anomalies (Ti/Ti* = 0.15–0.23; Hf/Hf* = 0.21–0.38).

3. Variations of Source Lithologies for Late Mesozoic Basalts

When crustal materials (i.e., oceanic crust) are subducted into the mantle, these mafic rocks transform into SiO_2-oversaturated eclogites. Such eclogite may melt first and produce residues of silica-deficient eclogites [*Hirschmann et al.*, 2003; *Kogiso et al.*, 2003; *Pertermann and Hirschmann*, 2003a, 2003b; *Yaxley and Green*, 1998]. In addition to these subducted mafic lithologies, the carbonate minerals, sequestered in oceanic crust by hydrothermal alteration, can also be introduced into the mantle [*Alt and Teagle*, 1999; *Jarrard*, 2003], based on the experimental solidus of carbonated eclogite [*Dasgupta et al.*, 2004; *Hammouda*, 2003] and the average subduction geotherm [*Peacock*, 2003; *van Keken et al.*, 2002]. Therefore, carbonated eclogite would be present in the upper mantle or even in the transition zone (or lower mantle) on account of oceanic slab subduction, and for the latter, carbonate would be present locally in oxidized domains. However, carbonated

eclogite delivered to the transition zone or lower mantle may eventually be returned to the upper mantle by convection. During this process, the solidus of carbonated eclogite [*Litasov and Ohtani*, 2010] would intersect the average mantle adiabat [*Akaogi et al*., 1989] at ~13–15 GPa. In this condition, carbonated eclogite is not stable in the upper part of upper mantle and would release a carbonatitic melt accompanying with the eclogite in the residue. Such melt would freeze during reactions with the surrounding mantle peridotite and produce the carbonated peridotite in the mantle [*Hammouda*, 2003]. Therefore, identifying the mantle lithologies of Late Mesozoic basalts at different stages can help us to understand the potential influence of paleo-Pacific plate subduction.

In order to assess the potential source lithology of Late Mesozoic mafic volcanic rocks, we need to calculate their primary magma compositions (Table S2), and therefore, we should first evaluate the possible fractionation process for these Mesozoic rocks, using the software "Petrolog 3" [*Danyushevsky and Plechov*, 2011]. As shown in Figure 1, at the beginning of fractional crystallization, olivine is the fractional mineral. The fractionation of olivine would decrease the Ni and MgO concentrations of melts because they are compatible in olivine [e.g., *Adam and Green*, 2006]. The CaO/Al_2O_3 ratios of melts are affected insignificantly during this stage. Then, because of the presence of clinopyroxene during fractionation, the CaO/Al_2O_3 ratios of melts are suggested to decrease significantly (Figure 1a). Additionally, if the plagioclase and orthopyroxene are removed before clinopyroxene during fractional crystallization, the CaO/Al_2O_3 ratios of melts would first increase slightly and then decrease (Figure 1a). The compatible of Al in plagioclase [e.g., *Aigner-Torres et al*., 2007] is the primary reason for the increasing of CaO/Al_2O_3 ratios during fractionation process. Based on the modeling of fractionation of different minerals, the correlation between Ni and MgO concentrations of most samples indicates the potential influence of fractional crystallization of olivine with other minerals (e.g., clinopyroxene or orthopyroxene). The Daoxian basalts show obviously high MgO (14.5–16.2 wt %) and Ni (503–818 ppm) concentrations with a large portion of olivine grains (almost ~20% [*Yang et al*., 2015]), strongly suggesting olivine accumulation for these basalts. Additionally, lack of negative Eu anomalies ($Eu/Eu^* = 0.96–1.16$; not shown) for those samples with relatively high MgO concentrations (>7.5 wt %) indicates no significant removal of plagioclase. Because Ca is compatible ($D^{Ca} = 1.33–5.31$) but Al is incompatible ($D^{Al} = 0.26–0.60$) in clinopyroxene [*Hill et al*., 2011], the fractionation of clinopyroxene can induce markedly decreased CaO/Al_2O_3 ratio with decreasing MgO content for magma. Therefore, those samples with relatively high MgO concentrations (>7.5 wt %) are also suggested to undergo negligible fractionation of clinopyroxene (Figure 1a) and are then chosen to be corrected, such that they are in equilibrium with an olivine composition of Fo_{90} by adding or subtracting olivine, following *Huang and Frey* [2003]: (1) the composition of equilibrium olivine was obtained using $K_D(Fe^{2+}/Mg)^{olivine/melt} = 0.3$ [*Roeder and Emslie*, 1970], assuming that 10% of the total iron are Fe^{3+} in the melt; (2) a more primitive basalt composition was calculated as a mixture of the basalt and equilibrium olivine in a weight ratio of 99.9:0.1; and (3) steps (1) and (2) were repeated until calculated equilibrium olivine had a Fo value of 90.

The calculated primary magmas of basalts from Daoxian (approximately 150 Ma) have formed along the cotectic L + Cpx + Grt (Figure 2a), indicating that the source lithology of these basalts is SiO_2-rich pyroxenite. Furthermore, comparing to the previous melting experimental results (Figures 2a and 2b), the source lithology for Daoxian basalts seems to have been carbonated, because carbonated components can provide higher CaO concentrations to the melts (Figure 2b). Previous studies on Cenozoic basalts from Shandong Provinces have summarized the chemical characteristics for those magmas derived from the carbonated source, including significantly negative anomalies of Zr, Hf, and Ti (i.e., low Ti/Ti* and Hf/Hf* ratios), high Zr/Hf and Ca/Al ratios [*Zeng et al*., 2010], which are then verified via the studies on Mg and Zn isotopes of basalts [e.g., *Huang et al*., 2015; *S.-A. Liu et al*., 2016; *Tian et al*., 2016]. For Daoxian basalts, they show significantly higher CaO/Al_2O_3 ratios and lower Hf/Hf* and Ti/Ti* ratios (Figure 3), suggesting the possible influence of carbonated components in the source. In the primitive-mantle-normalized incompatible element diagram (Figure S3; the primitive mantle values are from *McDonough and Sun* [1995]), the Daoxian basalts also display significantly negative anomalies of Zr, Hf, and Ti. Additionally, their Zr/Hf ratios (37.4–50.5) are higher than the value of chondrite [*Anders and Grevesse*, 1989]. All these characteristics are accordant with the "carbonatitic fingerprints." Therefore, we argue that the carbonated SiO_2-rich eclogite/pyroxenite can be an appropriated candidate for the source of Daoxian basalts.

By comparison, the primary magmas of those 178~172 Ma and 109~64 Ma basalts have formed along the cotectic L + Ol + Cpx + Grt (Figure 2a). In this area, peridotite or SiO_2-poor pyroxenite can be the candidate

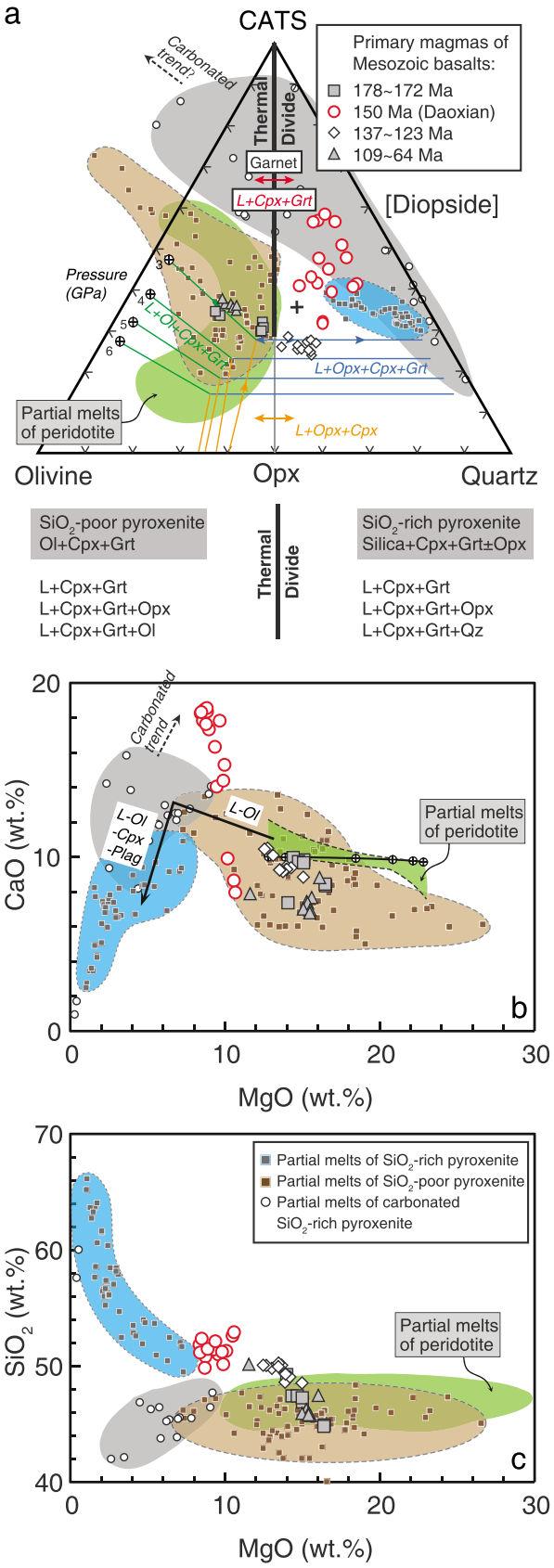

of their source lithology. The low CaO contents (CaO = 6.8–9.9 wt %) in primary magmas for these basalts (Figure 2b) supports a pyroxenitic residue rather than a peridotitic residue in the mantle source, because primary magmas from peridotite at pressures up to 7 GPa have significantly higher CaO contents (~10 wt %), regardless of the degree of fertility of the peridotite being melted [*Herzberg and Asimow*, 2008]. Additionally, they are plotted in the field of experimental partial melts of SiO_2-poor pyroxenite (Figure 2b), which also support the proposal of genesis of SiO_2-poor pyroxenite. For 137~123 Ma basalts, their source lithology seems to be related to SiO_2-rich pyroxenite because they have formed along the cotectic L + Opx + Cpx + Grt (Figure 2a). However, comparing to the melting experimental results, they are plotted far from the SiO_2-rich pyroxenite area (Figures 2b and 2c), which make their genesis puzzled. Interestingly, they

Figure 2. (a) Projections (mol %) of primary magmas for Late Mesozoic basalts in southeastern China from or toward diopside into the plane Olivine-Quartz-Calcium Tschermak's (CATS). The cotectic (L + Ol + Cpx + Opx), (L + Opx + Cpx + Grt), (L + Cpx + Grt), and (L + Opx + Cpx) constrained by the pressure (GPa), the thermal divide, and the area for oceanic crust and mantle peridotite are from *Herzberg* [2011]. The mole percent projection is derived from the code given by *O'Hara* [1968]. (b) Variations of CaO versus MgO of primary magmas for Late Mesozoic basalts in southeastern China. The fractionation trend (black arrow) and the area for primary melts from peridotite at 2–7 GPa (green field) are from *Herzberg and Asimow* [2008]. (c) Variations of SiO_2 versus MgO of primary magmas for Late Mesozoic basalts in southeastern China. Data source for experimental partial melts of SiO_2-rich and SiO_2-poor pyroxenite are after *Herzberg* [2011] and *Mallik and Dasgupta* [2014]. Also shown are the experimental partial melts of carbonated SiO_2-rich pyroxenite [*Gerbode and Dasgupta*, 2010; *Kiseeva et al.*, 2012] and peridotite [*Grove et al.*, 2013; *Walter*, 1998]. The primary magma compositions of Late Mesozoic basalts (MgO > 7.5 wt %; Table S2 in the supporting information) in this study are calculated by adding olivine, following *Huang and Frey* [2003]. Other data sources are the same as in Figure 1.

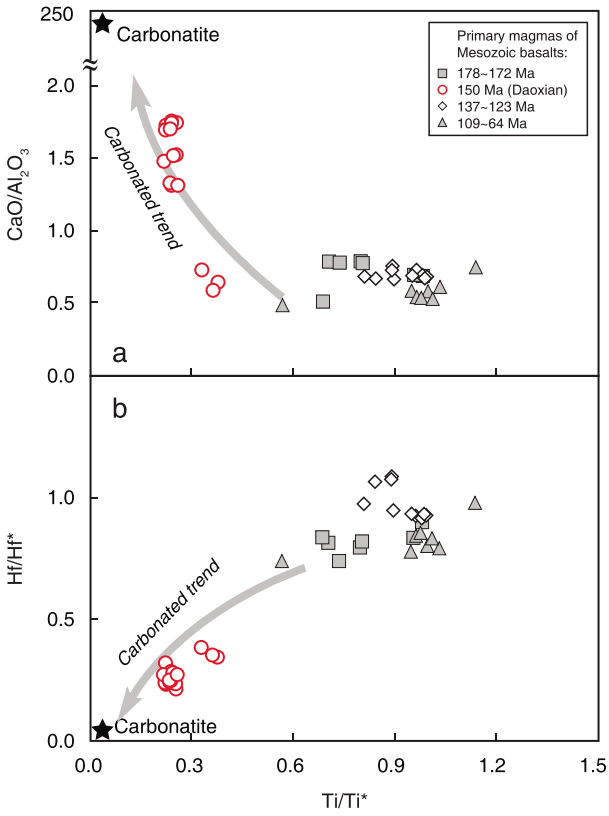

Figure 3. Variations in (a) CaO/Al_2O_3 and (b) Hf/Hf* versus Ti/Ti* for primary magmas of the Late Mesozoic basalts in southeastern China. Element anomalies are calculated as follows: $Hf/Hf^* = Hf_N/(Sm_N \times Nd_N)^{0.5}$ and $Ti/Ti^* = Ti_N/(Nd_N^{-0.055} \times Sm_N^{0.333} \times Gd_N^{0.722})$. The average values for carbonatites are based on data for oceanic magnesio-carbonatite from Cape Verdes [*Hoernle et al.*, 2002]. Data sources are the same as in Figure 1.

are always plotted in the area between Daoxian basalts and 178~172 Ma basalts. A possible explanation is that these 137~123 Ma basalts originated from a mixing mantle source. In addition to carbonated SiO_2-rich pyroxenite derived from the subducted paleo-Pacific plate, the SiO_2-poor pyroxenite, which represents the previous component in the mantle, also participated in the formation of these basalts.

In summary, we suggest that the pyroxenite is the principal lithology in the mantle source of Late Mesozoic basalts in southeastern China. In comparing to a SiO_2-poor pyroxenite for the basalts erupted in 178~172 Ma and 109~64 Ma, the source of basalts erupted in approximately 150 Ma and 137~123 Ma is mostly likely to be the SiO_2-rich pyroxenite (Figure 2).

4. Implication for the Geodynamics of Paleo-Pacific Plate Subduction

To further evaluate our speculation on source lithologies for Late Mesozoic basalts, we also performed the rare earth element modeling of mantle melting with different source lithologies (Figure 4). The La/Yb and Sm/Yb ratios of the basalts are controlled by both the mantle source and partial melting process. Based on the calculated results (Figure 4), we argue that carbonated components play important roles in the formation of these basalts because the presence of small amounts of carbonated components can increase the La/Yb ratios of basaltic magmas significantly. Most basalts cannot present the so-called carbonatitic fingerprints because they are diluted during the high degree of melting. Although we can hardly identify the source lithologies of samples with high melting degree (probably with La/Yb < 10), low-degree melting of mantle with different lithologies will produce melts with different La/Yb and Sm/Yb ratios. For those basalts from Daoxian, only the melting of carbonated, SiO_2-rich pyroxenite can well explain their significantly high La/Yb and Sm/Yb ratios (Figure 4). The possible reason for higher La/Yb and Sm/Yb ratios of melts from SiO_2-rich pyroxenite than melts from peridotite or SiO_2-poor pyroxenite is that the melting residues of SiO_2-rich pyroxenite have higher proportions of garnet, because Yb is strongly compatible in garnet ($D^{Yb} = 6.5–7.9$) during mantle partial melting [e.g., *Green et al.*, 2000; *Zack et al.*, 1997].

The Late Mesozoic igneous magmatism in southeastern China has long been attributed to the subduction of the paleo-Pacific plate [e.g., *Chen et al.*, 2008; *Jahn*, 1974; *Jahn et al.*, 1990; *Li and Li*, 2007; *Li et al.*, 2014; *Zhou and Li*, 2000; *Zhou et al.*, 2006], although the beginning time for the subducted paleo-Pacific plate affecting the mantle is still ambiguous. In this case, our studies on source lithology of Late Mesozoic basalts provide here important clues to understand the potential influence of such subducted slab in the mantle. The source lithology of 178~172 Ma basalts is a SiO_2-poor pyroxenite (Figure 2), formed from the reaction between recycled crust-derived melt and nearby peridotite (or carbonated peridotite-derived melt) [*Herzberg*, 2011; *Mallik and Dasgupta*, 2014; *Sobolev et al.*, 2005, 2007]. Such recycled crustal material can be either ancient or young, and their origin can hardly be distinguished. Then, a carbonated eclogite is proposed in the mantle

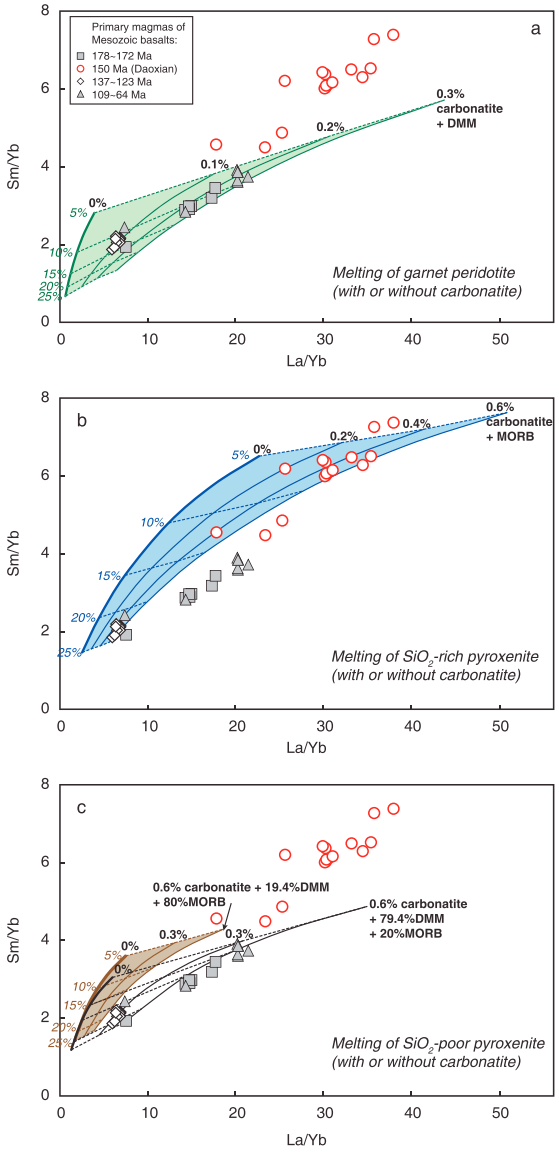

Figure 4. Variations in Sm/Yb versus La/Yb for primary magmas of the Late Mesozoic basalts in southeastern China. Also shown is the simple batch melting curve calculated for (a) garnet peridotite, (b) SiO_2-rich pyroxenite, and (c) SiO_2-poor pyroxenite with or without carbonatite. The black numbers represent the assumed proportion of the carbonatite in the source, while the colored numbers represent the partial melting degree. The proportion of carbonatite in the asthenospheric mantle is suggested to be less than 0.4% based on the study of electrical conductivity [*Gaillard et al.*, 2008], and we therefore assumed that the proportion of carbonatite ranges from 0% to 0.6% (slightly larger than 0.4%) in order to understand the potential influence of carbonated components on the Sm/Yb and La/Yb of basaltic melts from different mantle source. Additionally, during the calculation of SiO_2-poor pyroxenite, the proportion of MORB is selected as 80% and 20%, respectively, which can help us to understand the potential influence of increased degree of the reaction between recycled SiO_2-rich pyroxenite and nearby peridotite during the formation of SiO_2-poor pyroxenite. Partition coefficients for La, Sm, and Yb between cpx, grt, and melt during melting of SiO_2-rich pyroxenite are taken from *Zack et al.* [1997]. The proportions of residual phase (80% cpx and 20% grt) and melting reaction of SiO_2-rich pyroxenite (20% cpx and 80% grt) are assumed to be modal. Partition coefficients for La, Sm, and Yb between ol and melt during melting of garnet peridotite and SiO_2-poor pyroxenite are taken from *Zanetti et al.* [2004]; partition coefficients for La, Sm, and Yb between cpx, opx, grt, and melt are taken from *Green et al.* [2000]. The proportions of residual phase during partial melting of garnet peridotite (62% ol, 18% cpx, 15% opx, and 5% grt) and SiO_2-poor pyroxenite (20% ol, 24% cpx, 54% opx, and 2% grt) are assumed to be modal. Melting reaction of garnet peridotite (<50% partial melting: 3% ol, 70% cpx, 3% opx, and 24% grt) is after *Walter* [1998]. Melting reaction of SiO_2-poor pyroxenite (<18% partial melting: 46% ol, 51% cpx, −3% opx, and 6% grt; 18~35% partial melting: 44% ol, 73% cpx, −30% opx, and 13% grt) is after *Longhi* [2002]. The data for depleted MORB mantle (DMM) and average MORB are from *Workman and Hart* [2005] and *Niu et al.* [1999]. The average values for carbonatites are based on data for oceanic magnesio-carbonatite from Cape Verdes [*Hoernle et al.*, 2002]. Data sources are the same as in Figure 1.

source of approximately 150 Ma Daoxian basalts (Figures 2–4). This may indicate that a carbonated, SiO_2-rich material is introduced into the mantle around this period. Such material cannot be the ancient recycled crustal components because the carbonated eclogite cannot be preserved in the upper part of upper mantle during ascent based on the solidus of carbonated eclogite [*Litasov and Ohtani*, 2010] and the average mantle adiabat [*Akaogi et al*., 1989]. Therefore, we suggest that the subducted paleo-Pacific plate is the most appropriate candidate for such carbonated eclogite. Because rutile is a common accessory phase in the subducted slab and Nb is highly compatible in rutile [*Foley et al*., 2000; *Klemme et al*., 2005], obviously negative anomalies of Nb for Daoxian basalts (Figure S3) also support the melting of such eclogite with the residue of rutile. In other words, the subducted plate has reached the area beneath Hunan Province at approximately 150 Ma and is responsible for the mantle-derived magmatism after this period. A mixing, SiO_2-rich pyroxenite-bearing source (Figures 2 and 4) for those 137~123 Ma basalts also supports the persistent influence of the subducted paleo-Pacific plate in the formation of mantle-derived magma, although most carbonatitic fingerprints might have been diluted by the increased melting degree for these basalts (Figure 4b). Such influence becomes to be negligible for the 109~64 Ma basalts since their source lithology is transformed into the SiO_2-poor pyroxenite in this stage. The lithological variations of mantle can be explained using the model of a paleo-Pacific slab rollback with increased dip angle, which is consistent with evidence from syenitic, gabbroic, granitic, and volcanic rocks in southeastern China [*He and Xu*, 2012; *Jiang et al*., 2009; *L. Liu et al*., 2016]. Before 150 Ma, the subducted paleo-Pacific slab has not affected the mantle source of Mesozoic rocks and the mantle is composed mainly by the peridotite and SiO_2-poor pyroxenite; the latter, which has been suggested to play an important role in the generation of mantle-derived, basaltic magma [e.g., *Keshav et al*., 2004; *Kogiso and Hirschmann*, 2004; *Kogiso et al*., 2003; *Mallik and Dasgupta*, 2012, 2013; *Pertermann and Hirschmann*, 2003a, 2003b; *Yaxley and Green*, 1998], is mostly likely to be produced by the reaction between ancient recycled crustal material-derived melt and nearby peridotite [*Herzberg*, 2011; *Sobolev et al*., 2005, 2007]. After 150 Ma, the subducted paleo-Pacific slab reached the area which approximately corresponds to the present Hunan Province and begun to affect the mantle-derived magmatism until 110 Ma. Due to the increasing of dip angle for subducted slab induced by the growing gravity [e.g., *Niu*, 2014], the entire southeastern China was under back-arc extensional setting after 110 Ma [*Li and Li*, 2007; *Lui et al*., 2014a, 2014b; *Pearce and Stern*, 2006; *Zhou et al*., 2006], and mantle-derived magma in this period shows the principal affinity of asthenospheric mantle again [*Meng et al*., 2012].

Acknowledgments

We appreciate the thoughtful and constructive review provided by Ananya Mallik and Editor Jeroen Ritsema. This study was supported by National Basic Research Program of China (2012CB416701) and the National Natural Science Foundation of China (grants 41430208, 41672048, and 41302044).

References

Adam, J., and T. Green (2006), Trace element partitioning between mica- and amphibole-bearing garnet lherzolite and hydrous basanitic melt: 1. Experimental results and the investigation of controls on partitioning behavior, *Contrib. Mineral. Petrol.*, *152*, 1–17.

Aigner-Torres, M., J. D. Blundy, P. Ulmer, and T. Pettke (2007), Laser Ablation ICPMS study of trace element partitioning between plagioclase and basaltic melts: An experimental approach, *Contrib. Mineral. Petrol.*, *153*, 647–667.

Akaogi, M., E. Ito, and A. Navrotsky (1989), Olivine-modified spinel-spinel transitions in the system Mg_2SiO_4-Fe_2SiO_4: Calorimetric measurements, thermochemical calculation, and geophysical application, *J. Geophys. Res.*, *94*, 15,671–15,685, doi:10.1029/JB094iB11p15671.

Alt, J. C., and D. A. Teagle (1999), The uptake of carbon during alteration of ocean crust, *Geochim. Cosmochim. Acta*, *63*, 1527–1535.

Anders, E., and N. Grevesse (1989), Abundances of the elements: Meteoritic and solar, *Geochim. Cosmochim. Acta*, *53*, 197–214.

Chen, C.-H., C.-Y. Lee, and R. Shinjo (2008), Was there Jurassic paleo-Pacific subduction in South China?: Constraints from $^{40}Ar/^{39}Ar$ dating, elemental and Sr–Nd–Pb isotopic geochemistry of the Mesozoic basalts, *Lithos*, *106*, 83–92.

Dai, B. Z. (2007), Geochronology and geochemistry of the Mesozoic mafic magmatisms in southern Hunan Province, China: Implications for multi-stage lithospheric extension in south China, Doctor thesis, pp. 1–141, Nanjing Univ., Nanjing.

Danyushevsky, L. V., and P. Plechov (2011), Petrolog3: Integrated software for modeling crystallization processes, *Geochem. Geophys. Geosyst.*, *12*, Q07021, doi:10.1029/2011GC003516.

Dasgupta, R., M. M. Hirschmann, and A. C. Withers (2004), Deep global cycling of carbon constrained by the solidus of anhydrous, carbonated eclogite under upper mantle conditions, *Earth Planet. Sci. Lett.*, *227*, 73–85.

Dasgupta, R., M. G. Jackson, and C. T. Lee (2010), Major element chemistry of ocean island basalts—Conditions of mantle melting and heterogeneity of mantle source, *Earth Planet. Sci. Lett.*, *289*, 377–392.

Foley, S. F., M. G. Barth, and G. A. Jenner (2000), Rutile/melt partition coefficients for trace elements and an assessment of the influence of rutile on the trace element characteristics of subduction zone magmas, *Geochim. Cosmochim. Acta*, *64*, 933–938.

Gaillard, F., M. Malki, G. Lacono-Marziano, M. Pichavant, and B. Scaillet (2008), Carbonatite melts and electrical conductivity in the asthenosphere, *Science*, *322*, 1363–1365, doi:10.1126/science.1164446.

Gerbode, C., and R. Dasgupta (2010), Carbonate-fluxed melting of MORB-like pyroxenite at 2.9 GPa and genesis of HIMU ocean island basalts, *J. Petrol.*, *51*, 2067–2088.

Green, T. H., J. D. Blundy, J. Adam, and G. M. Yaxley (2000), SIMS determination of trace element partition coefficients between garnet, clinopyroxene and hydrous basaltic liquids at 2–7.5 GPa and 1080–1200 °C, *Lithos*, *53*, 165–187.

Grove, T. L., E. S. Holbig, J. A. Barr, C. B. Till, and M. J. Krawczynski (2013), Melts of garnet lherzolite: Experiments, models and comparison to melts of pyroxenite and carbonated lherzolite, *Contrib. Mineral. Petrol.*, *166*, 887–910.

Hammouda, T. (2003), High-pressure melting of carbonated eclogite and experimental constraints on carbon recycling and storage in the mantle, *Earth Planet. Sci. Lett.*, *214*, 357–368.
He, Z.-Y., and X.-S. Xu (2012), Petrogenesis of the Late Yanshanian mantle-derived intrusions in southeastern China: Response to the geodynamics of paleo-Pacific plate subduction, *Chem. Geol.*, *328*, 208–221.
Herzberg, C. (2006), Petrology and thermal structure of the Hawaiian plume from Mauna Kea volcano, *Nature*, *444*, 605–609.
Herzberg, C. (2011), Identification of source lithology in the Hawaiian and Canary islands: Implications for origins, *J. Petrol.*, *52*, 113–146, doi:10.1093/petrology/egq075.
Herzberg, C., and P. D. Asimow (2008), Petrology of some oceanic island basalts: PRIMELT2.XLS software for primary magma calculation, *Geochem. Geophys. Geosyst.*, *9*, Q09001, doi:10.1029/2008GC002057.
Hill, E., J. Blundy, and B. Wood (2011), Clinopyroxene–melt trace element partitioning and the development of a predictive model for HFSE and Sc, *Contrib. Mineral. Petrol.*, *161*, 423–438, doi:10.1007/s00410-010-0540-0.
Hirschmann, M. M., T. Kogiso, M. B. Baker, and E. M. Stolper (2003), Alkalic magmas generated by partial melting of garnet pyroxenite, *Geology*, *31*, 481–484.
Hoernle, K., G. Tilton, M. J. Le Bas, S. Duggen, and D. Garbe-Schonberg (2002), Geochemistry of oceanic carbonatites compared with continental carbonatites: Mantle recycling of oceanic crustal carbonate, *Contrib. Mineral. Petrol.*, *142*, 520–542.
Huang, J., S.-G. Li, Y. Xiao, S. Ke, W.-Y. Li, and Y. Tian (2015), Origin of low δ^{26}Mg Cenozoic basalts from South China Block and their geodynamic implications, *Geochim. Cosmochim. Acta*, *164*, 298–317, doi:10.1016/j.gca.2015.04.054.
Huang, S., and F. A. Frey (2003), Trace element abundances of Mauna Kea basalt from phase 2 of the Hawaii Scientific Drilling Project: Petrogenetic implications of correlations with major element content and isotopic ratios, *Geochem. Geophys. Geosyst.*, *4*(6), 8711, doi:10.1029/2002GC000322.
Jahn, B.-M. (1974), Mesozoic thermal events in southeast China, *Nature*, *248*, 480–483.
Jahn, B. M., X. H. Zhou, and J. L. Li (1990), Formation and tectonic evolution of southeastern China and Taiwan: Isotopic and geochemical constraints, *Tectonophysics*, *183*, 145–160.
Jarrard, R. D. (2003), Subduction fluxes of water, carbon dioxide, chlorine, and potassium, *Geochem. Geophys. Geosyst.*, *4*(5), 8905, doi:10.1029/2002GC000392.
Jiang, Y.-H., S.-Y. Jiang, B.-Z. Dai, S.-Y. Liao, K.-D. Zhao, and H.-F. Ling (2009), Middle to Late Jurassic felsic and mafic magmatism in southern Hunan Province, southeast China: Implications for a continental arc to rifting, *Lithos*, *107*, 185–204.
Keshav, S., G. H. Gudfinnsson, G. Sen, and Y.-W. Fei (2004), High-pressure melting experiments on garnet clinopyroxenite and the alkalic to tholeiitic transition in ocean-island basalts, *Earth Planet. Sci. Lett.*, *223*, 365–379.
Kiseeva, E. S., G. M. Yaxley, J. Hermann, K. D. Litasov, A. Rosenthal, and V. S. Kamenetsky (2012), An experimental study of carbonated eclogite at 3 · 5–5 · 5 GPa—Implications for silicate and carbonate metasomatism in the cratonic mantle, *J. Petrol.*, *53*, 727–759, doi:10.1093/petrology/egr078.
Klemme, S., S. Prowatke, K. Hametner, and D. Günther (2005), Partitioning of trace elements between rutile and silicate melts: Implications for subduction zones, *Geochim. Cosmochim. Acta*, *69*, 2361–2371.
Klimetz, M. P. (1983), Speculations on the Mesozoic plate tectonic evolution of eastern China, *Tectonics*, *2*, 139–166, doi:10.1029/TC002i002p00139.
Kogiso, T., and M. M. Hirschmann (2004), High-pressure partial melting of mafic lithologies in the mantle, *J. Petrol.*, *45*, 2407–2422.
Kogiso, T., M. M. Hirschmann, and D. J. Frost (2003), High-pressure partial melting of garnet pyroxenite: Possible mafic lithologies in the source of ocean island basalts, *Earth Planet. Sci. Lett.*, *216*, 603–617.
Le Bas, M., R. Le Maitre, A. Streckeisen, and B. Zanettin (1986), A chemical classification of volcanic rocks based on the total alkali-silica diagram, *J. Petrol.*, *27*, 745–750.
Li, X.-H., S.-L. Chung, H. Zhou, C.-H. Lo, Y. Liu, and C.-H. Chen (2004), Jurassic intraplate magmatism in southern Hunan-eastern Guangxi: ^{40}Ar/^{39}Ar dating, geochemistry, Sr-Nd isotopes and implications for the tectonic evolution of SE China, in *Aspects of the Tectonic Evolution of China*, vol. 226, edited by J. Malpas et al., pp. 193–215, Geol. Soc. London, London.
Li, Z., J.-S. Qiu, and X.-M. Yang (2014), A review of the geochronology and geochemistry of Late Yanshanian (Cretaceous) plutons along the Fujian coastal area of southeastern China: Implications for magma evolution related to slab break-off and rollback in the Cretaceous, *Earth Sci. Rev.*, *128*, 232–248.
Li, Z.-X., and X.-H. Li (2007), Formation of the 1300-km-wide intracontinental orogen and postorogenic magmatic province in Mesozoic south China: A flat-slab subduction model, *Geology*, *35*, 179–182.
Litasov, K., and E. Ohtani (2010), The solidus of carbonated eclogite in the system CaO-Al_2O_3-MgO-SiO_2-Na_2O-CO_2 to 32 GPa and carbonatite liquid in the deep mantle, *Earth Planet. Sci. Lett.*, *295*, 115–126.
Liu, L., X. Xu, and Y. Xia (2014a), Cretaceous Pacific plate movement beneath SE China: Evidence from episodic volcanism and related intrusions, *Tectonophysics*, *614*, 170–184.
Liu, L., J.-S. Qiu, J.-L. Zhao, and Z.-L. Yang (2014b), Geochronological, geochemical, and Sr–Nd–Hf isotopic characteristics of Cretaceous monzonitic plutons in western Zhejiang Province, southeast China: New insights into the petrogenesis of intermediate rocks, *Lithos*, *196*, 242–260.
Liu, L., X. Xu, and Y. Xia (2016), Asynchronizing paleo-Pacific slab rollback beneath SE China: Insights from the episodic Late Mesozoic volcanism, *Gondwana Res.*, doi:10.1016/j.gr.2015.09.009.
Liu, S.-A., Z.-Z. Wang, S.-G. Li, J. Huang, and W. Yang (2016), Zinc isotope evidence for a large-scale carbonated mantle beneath eastern China, *Earth Planet. Sci. Lett.*, *444*, 169–178, doi:10.1016/j.epsl.2016.03.051.
Longhi, J. (2002), Some phase equilibrium systematics of lherzolite melting: I, *Geochem. Geophys. Geosyst.*, *3*(3), 1020, doi:10.1029/2001GC000204.
Mallik, A., and R. Dasgupta (2012), Reaction between MORB-eclogite derived melts and fertile peridotite and generation of ocean island basalts, *Earth Planet. Sci. Lett.*, *329*, 97–108, doi:10.1016/j.epsl.2012.02.007.
Mallik, A., and R. Dasgupta (2013), Reactive infiltration of MORB-eclogite-derived carbonated silicate melt into fertile peridotite at 3 GPa and genesis of alkalic magmas, *J. Petrol.*, *54*, 2267–2300, doi:10.1093/petrology/egt047.
Mallik, A., and R. Dasgupta (2014), Effect of variable CO_2 on eclogite-derived andesite and lherzolite reaction at 3 GPa—Implications for mantle source characteristics of alkalic ocean island basalts, *Geochem. Geophys. Geosyst.*, *15*, 1533–1557, doi:10.1002/2014GC005251.
McDonough, W. F., and S. S. Sun (1995), The composition of the Earth, *Chem. Geol.*, *120*, 223–253.
Meng, L., Z.-X. Li, H. Chen, X.-H. Li, and X.-C. Wang (2012), Geochronological and geochemical results from Mesozoic basalts in southern South China Block support the flat-slab subduction model, *Lithos*, *132*, 127–140.

Niu, Y. (2014), Geological understanding of plate tectonics: Basic concepts, illustrations, examples and new perspectives, *Global Tectonics Metallogeny*, *10*, 23–46.
Niu, Y., K. D. Collerson, R. Batiza, I. J. Wendt, and M. Regelous (1999), Origin of E-type MORB at ridges far from mantle plumes: The East Pacific Rise at 11°20′, *J. Geophys. Res.*, *104*, 7067–7087, doi:10.1029/1998JB900037.
O'Hara, M. J. (1968), The bearing of phase equilibria studies in synthetic and natural systems on the origin of basic and ultrabasic rocks, *Earth Sci. Rev.*, *4*, 69–133.
Peacock, S. M. (2003), Thermal structure and metamorphic evolution of subducting slabs, in *Inside the Subduction Factory*, edited by J. M. Eiler, pp. 7–22, AGU, Washington, D. C.
Pearce, J. A., and R. J. Stern (2006), Origin of back-arc basin magmas: Trace element and isotope perspectives, in *Back-Arc Spreading Systems: Geological, Biological, Chemical, and Physical Interactions*, vol. 166, edited by D. M. Christie et al., pp. 63–86, AGU, Washington, D. C.
Pertermann, M., and M. M. Hirschmann (2003a), Partial melting experiments on a MORB-like pyroxenite between 2 and 3 GPa: Constraints on the presence of pyroxenite in basalt source regions from solidus location and melting rate, *J. Geophys. Res.*, *108*(B2), 2125, doi:10.1029/2000JB000118.
Pertermann, M., and M. M. Hirschmann (2003b), Anhydrous partial melting experiment on MORB-like eclogites phase relations, phase composition and mineral-melt partitioning of major elements at 2–3 GPa, *J. Petrol.*, *44*, 2173–2202.
Pilet, S., M. B. Baker, and E. M. Stolper (2008), Metasomatized lithosphere and the origin of alkaline lavas, *Science*, *320*, 916–919, doi:10.1126/science.1156563.
Roeder, P. L., and R. F. Emslie (1970), Olivine-liquid equilibrium, *Contrib. Mineral. Petrol.*, *29*, 275–289, doi:10.1007/bf00371276.
Sobolev, A. V., A. W. Hofmann, S. V. Sobolev, and I. K. Nikogosian (2005), An olivine-free mantle source of Hawaiian shield basalts, *Nature*, *434*, 590–597.
Sobolev, A. V., et al. (2007), The amount of recycled crust in sources of mantle-derived melts, *Science*, *316*, 412–417.
Tian, H., W. Yang, S.-G. Li, S. Ke, and Z. Chu (2016), Origin of low δ^{26}Mg basalts with EM-I component: Evidence for interaction between enriched lithosphere and carbonated asthenosphere, *Geochim. Cosmochim. Acta*, doi:10.1016/j.gca.2016.05.021.
van Keken, P. E., B. Kiefer, and S. M. Peacock (2002), High-resolution models of subduction zones: Implications for mineral dehydration reactions and the transport of water into the deep mantle, *Geochem. Geophys. Geosyst.*, *3*(10), 1056, doi:10.1029/2001GC000256.
Walter, M. J. (1998), Melting of garnet peridotite and the origin of komatiite and depleted lithosphere, *J. Petrol.*, *39*, 29–60.
Wang, Y., W. Fan, F. Guo, T. Peng, and C. Li (2003), Geochemistry of Mesozoic mafic rocks adjacent to the Chenzhou-Linwu Fault, south China: Implications for the lithospheric boundary between the Yangtze and Cathaysia Blocks, *Int. Geol. Rev.*, *45*, 263–286.
Wang, Y., W. Fan, P. A. Cawood, and S. Li (2008), Sr–Nd–Pb isotopic constraints on multiple mantle domains for Mesozoic mafic rocks beneath the South China Block hinterland, *Lithos*, *106*, 297–308.
Wang, Y., Z. F. Zhao, Y. F. Zheng, and J. J. Zhang (2011), Geochemical constraints on the nature of mantle source for Cenozoic continental basalts in east-central China, *Lithos*, *125*, 940–955, doi:10.1016/j.lithos.2011.05.007.
Workman, R. K., and S. R. Hart (2005), Major and trace element composition of the depleted MORB mantle (DMM), *Earth Planet. Sci. Lett.*, *231*, 53–72, doi:10.1016/j.epsl.2004.12.005.
Xu, Y. G., H. H. Zhang, H. N. Qiu, W. C. Ge, and F. Y. Wu (2012a), Oceanic crust components in continental basalts from Shuangliao, northeast China: Derived from the mantle transition zone? *Chem. Geol.*, *328*, 168–184, doi:10.1016/j.chemgeo.2012.01.027.
Xu, Z., Z. F. Zhao, and Y. F. Zheng (2012b), Slab–mantle interaction for thinning of cratonic lithospheric mantle in north China: Geochemical evidence from Cenozoic continental basalts in central Shandong, *Lithos*, *146-147*, 202–217.
Yang, J. B., Z. D. Zhao, X. X. Mo, D. Sheng, C. Ding, L. L. Wang, Q. Y. Hou, and H. L. Li (2015), Petrogenesis and implications for alkali olivine basalts and its basic xenoliths from Huziyan in Dao County, Hunan Province, *Acta Petrol. Sin.*, *31*, 1421–1432.
Yaxley, G. M., and D. H. Green (1998), Reactions between eclogite and peridotite: Mantle refertilisation by subduction of oceanic crust, *Schweiz. Mineral. Petrogr. Mitt.*, *78*, 243–255.
Zack, T., S. F. Foley, and G. A. Jenner (1997), A consistent partition coefficient set for clinopyroxene, amphibole and garnet from laser ablation microprobe analysis of garnet pyroxenites from Kakanui, New Zealand, *Neues Jahrb. Mineral. Abhirchen*, *172*, 23–41.
Zanetti, A., M. Tiepolo, R. Oberti, and R. Vannucci (2004), Trace-element partitioning in olivine: Modelling of a complete data set from a synthetic hydrious basanite melt, *Lithos*, *75*, 39–54.
Zeng, G., L. H. Chen, X. S. Xu, S. Y. Jiang, and A. W. Hofmann (2010), Carbonated mantle sources for Cenozoic intra-plate alkaline basalts in Shandong, north China, *Chem. Geol.*, *273*, 35–45.
Zeng, G., L. H. Chen, A. W. Hofmann, S. Y. Jiang, and X. S. Xu (2011), Crust recycling in the sources of two parallel volcanic chains in Shandong, north China, *Earth Planet. Sci. Lett.*, *302*, 359–368, doi:10.1016/j.epsl.2010.12.026.
Zhou, X. M., and W. X. Li (2000), Origin of Late Mesozoic igneous rocks in southeastern China: Implications for lithosphere subduction and underplating of mafic magmas, *Tectonophysics*, *326*, 269–287.
Zhou, X. M., T. Sun, W. Z. Shen, L. S. Shu, and Y. L. Niu (2006), Petrogenesis of Mesozoic granitoids and volcanic rocks in South China: A response to tectonic evolution, *Episodes*, *29*, 26–33.